

Review Article

H¹ Magnetic Resonance Spectroscopy of Cystic Ovarian Lesions

Young Hye Kang¹, Mi Young Kim¹, Kyung Tae Kim¹, Yoon Jung Kim¹, Chang Hae Suh¹, Jun Mee Kim², Sung Ook Hwang³, Sunghyok Park⁴, Jae Young Cho⁵

¹Department of Radiology, Inha University School of Medicine

²Department of Pathology, Inha University School of Medicine

³Department of Gynecology, Inha University School of Medicine

⁴College of pharmacology, Seoul National University

⁵Biology, New York University

On H¹ MRS (magnetic resonance spectroscopy), malignant tumors show higher concentration of metabolite than benign lesions. Lactate double peak was detected in malignant tumor and endometriosis, and more prominent high concentration was demonstrated in endometriosis. Tuboovarian abscesses and salpingitis do not show prominent peak. Dermoid cysts show high levels of lipid peak. Paratubal cyst and follicular cyst can be showed the lipid peak, however, the concentration of lipid is lower than that of dermoid cyst. H¹ MRS of ovarian cystic lesions can give valuable information about the presence of metabolites of ovarian cystic lesions.

Index words : Ovary · Cyst · Cystic neoplasm · Magnetic resonance spectroscopy (MRS)

INTRODUCTION

Most female ovarian lesions manifest as cystic masses contain variable contents of fluid. MR image is increasingly used to evaluate these cystic lesions; malignancy can in some cases be predicted, however, sometimes it is nonspecific for differentiation of benign and malignant lesions. Solid component of ovarian cystic tumors visualized on ultrasonography, CT or MR images strongly supports the diagnosis for malignancy (1-4). Although the presence of tumor

markers (CA-125, CA15.9, CEA, CASA and CA 72-4) for the differential diagnosis of ovarian tumors has been studied, there is compelling evidence that cyst fluid tumor marker levels cannot distinguish adequately between the different histologic types. In vivo MRS (magnetic resonance spectroscopy) is a powerful and a noninvasive chemical analysis. This essay illustrated the use of MRS in evaluating female ovarian cystic lesions.

In vivo proton MRS was performed with a free-breathing multivoxel point-resolved spectroscopy (PRESS) sequence (TR/TE = 1500/135 msec or 1500/30 msec, 2048-point acquisition, 2500 Hz bandwidth eight averages). CHESS water suppression with 20 Hz bandwidth was obtained after semiautomated higher-order shimming. Outer volume suppression was achieved with six suppression bands placed three-dimensionally around the lesion. Post-processing was applied automatically with zero-order phase correction, zero-filling to 4096 points, and noise

• Received; October 7, 2013 • Revised; December 15, 2013

• Accepted; December 17, 2013

This work was supported by Inha University research grant.

Corresponding author : Mi Young Kim, M.D.

Department of Radiology, Inha University School of Medicine, Inhanro 27, Jung-gu, Incheon 400-711, Korea.

Tel. 82-32-890-2769, Fax. 82-32-890-2743

E-mail : mykim@inha.ac.kr

removal with a low pass 1.25 Hz Gaussian filter. The Voxel of interest for MRS measurement was placed at the center of the pelvic cystic lesions to avoid a contamination signal from adjacent normal tissue, and voxel size was approximately 1 cm³ or 8 cm³ depending on the tumor size. The data sets to a workstation operated on SA/GE software (GE). Prior to proton-MRS, pelvic CT or MRI findings were reviewed by a radiologist to determine the location of cystic lesions.

Benign and Malignant Epithelial tumor

Epithelial ovarian tumors can be classified as benign (60% of cases), malignant (35%), or borderline (low-

malignant-potential) (5%) depending on their histologic characteristics and clinical behaviors (3). Epithelial tumors are primarily cystic, which may be either unilocular or multilocular, and the malignant varieties are associated with varying proportions of a solid component.

In cases with benign and borderline epithelial tumor, there is no significantly prominent peak was not found (Fig. 1a) and consisted in low levels of lipid, lactate, glycoprotein. This also revealed MR spectrum around 2.05 ppm in cystic portion of benign and borderline neoplasms (Fig. 2 and 3). In study of cystic ovarian tumors, the high concentration of N-acetyl-L-aspartic

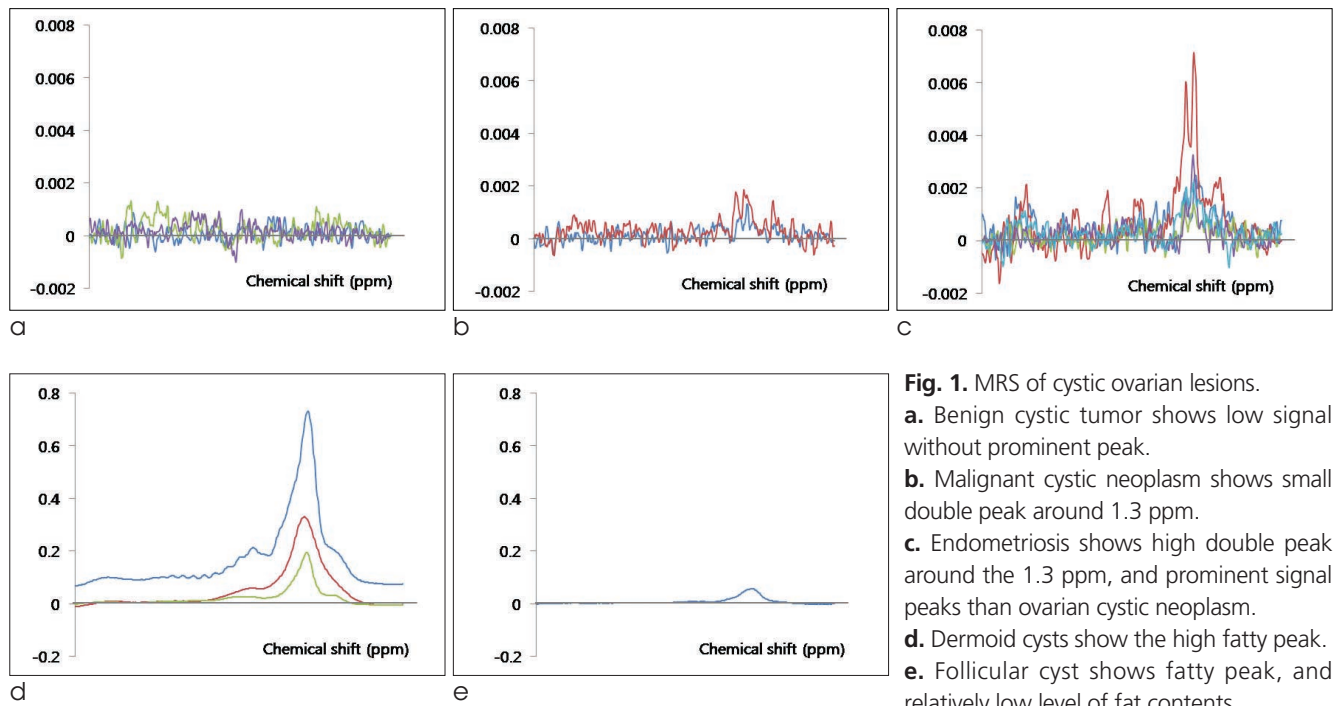


Fig. 1. MRS of cystic ovarian lesions. **a.** Benign cystic tumor shows low signal without prominent peak. **b.** Malignant cystic neoplasm shows small double peak around 1.3 ppm. **c.** Endometriosis shows high double peak around the 1.3 ppm, and prominent signal peaks than ovarian cystic neoplasm. **d.** Dermoid cysts show the high fatty peak. **e.** Follicular cyst shows fatty peak, and relatively low level of fat contents.

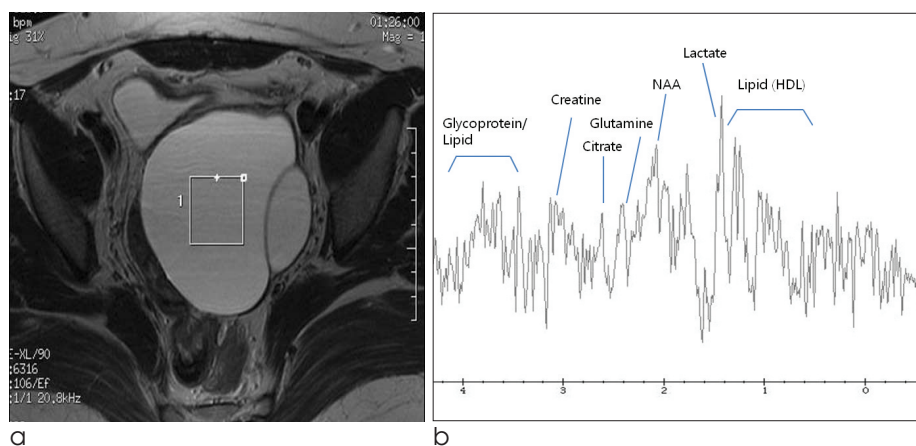


Fig. 2. 53-year-old women with serous cystadenoma (TR=3157 msec, TE=35 msec). **a.** Axial T2-weighted MR image shows a lesion of homogeneous hyperintense cystic mass without solid component. **b.** On MRS, there is no detectable peak.

acid (NAA) was confirmed in benign serous tumors, and they conclude that both NAA and N-acetyl groups from glycoproteins and/or glycolipids may contribute to the 2.0–2.1 ppm resonance complex in ovarian cyst fluid (5).

Compared to benign subtypes, significantly higher concentrations of leucine, valine, threonine, lactate, acetate, methionine, glutamine and choline and glycoprotein were detected in the malignant cyst fluid than in the benign cyst fluid (Fig. 4). Although the origin of the triglycerides is debated, cell growth retardation and cell death are likely to be responsible for the triglyceride peaks (6). Rapid cellular turnover in malignant tissues usually leads to a considerable amount of cellular deaths, resulting in areas of necrosis, which appear as a lipid signal. A high lipid peak indicates the disruption of macromolecules in the cell membrane of tumor cells in cases of brain and uterine cervix cancer (7, 8). On study of lung cancer, the paucity of lipid in normal lung parenchyma and

detection of lipid peak within the tumor on vivo MRS might play a role for the evaluation of cancer (9).

The doublet peak around 1.3 ppm represents lactate and lipid. Although lactate signals were detected even in some cases of benign tumor, all malignant tumors showed lactate peak and tended to form higher peaks than the benign tumors (10–12). The lactate signal reflects anaerobic glycolysis and there have been many reports that the lactate signal is higher in the malignant brain tumors (13). In specimens (Borrmann type III) with tubular adenocarcinoma, cancer lesions showed decreased levels of lipid peaks, significant levels of lactate doublet peaks, and increased intensity of the choline peak as compared with noncancerous gastric tissue (14).

Metastatic ovarian tumor

Metastatic ovarian tumor represents 5–15% of malignant ovarian tumors. Breast cancer, colon cancer, gastric cancer, and lymphoma are the most frequent

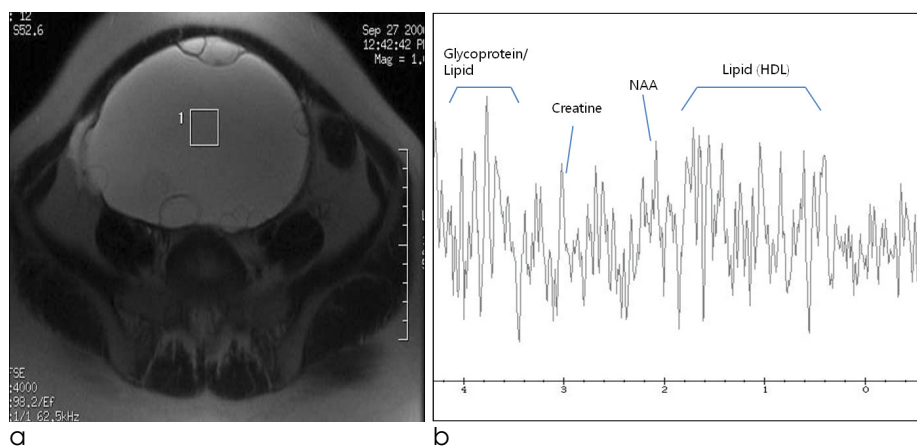


Fig. 3. 27-year-old woman with borderline mucinous tumor (TR=3157 msec, TE=35 msec).

- a.** Axial T2-weighted MR image shows a multilocular cystic lesion.
b. On MRS, there is no detectable peak.

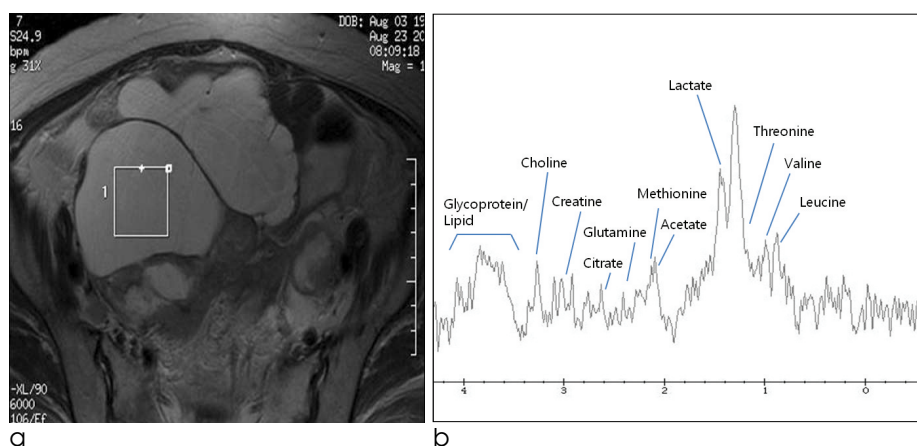


Fig. 4. 69-year-old woman with serous cystadenocarcinoma (TR = 3157 msec, TE=35 msec).

- a.** Axial T2-weighted MR image shows a septated cystic mass with thick septa and solid lesion.
b. On MRS, double peaks (asterisk) are observed around 1.3 ppm.

neoplasms to metastasize to the ovaries. Imaging findings in metastatic lesions are nonspecific solid and cystic lesion (2). In the study, two metastatic ovarian tumors are included: metastatic squamous cell carcinoma from uterine cervix and Krukenberg tumor from stomach. They showed double peaks around 1.3 ppm (Fig. 5). Like malignant epithelial tumor, higher concentrations of leucine, valine, threonine, lactate, acetoacetate, glutamine and choline and glycoprotein than benign epithelial tumor were detected. Hagberg et al. found higher serum concentrations of lactic acid in non-Hodgkin's lymphoma, significantly correlated with spread of the disease, as well as histological grade of malignancy (15). The observations in malignant cysts of high lactic acid and alanine in combination with low glucose, compared to benign cysts, seem to indicate a preference for anaerobic metabolism or an impairment of aerobic pathways in this cyst type (16). A significantly higher concentration of choline was also found in metastatic cyst fluids. Increased prolifer-

ation in malignancy resulting in increased membrane synthesis may form the basis of this high choline concentration (13).

In several types of cancer (including colorectal, gastric, breast, cervical, prostate, and ovarian), an unassigned and prominent resonance in the region from 2.0 to 2.1 ppm has been frequently found by MRS, and its intensity has often been associated with tumor invasion or malignancy (6, 14).

Mature cystic teratoma

Mature cystic teratomas are most common ovarian germ cell neoplasm and also the most common ovarian neoplasm in patients younger than 20 years. Mature cystic teratomas are composed of well-differentiated derivations from at least two of the three germ cell layers. At MR imaging, the sebaceous component of mature cystic teratomas has very high signal intensity on T1-weighted images, similar to retroperitoneal fat. The signal intensity of the

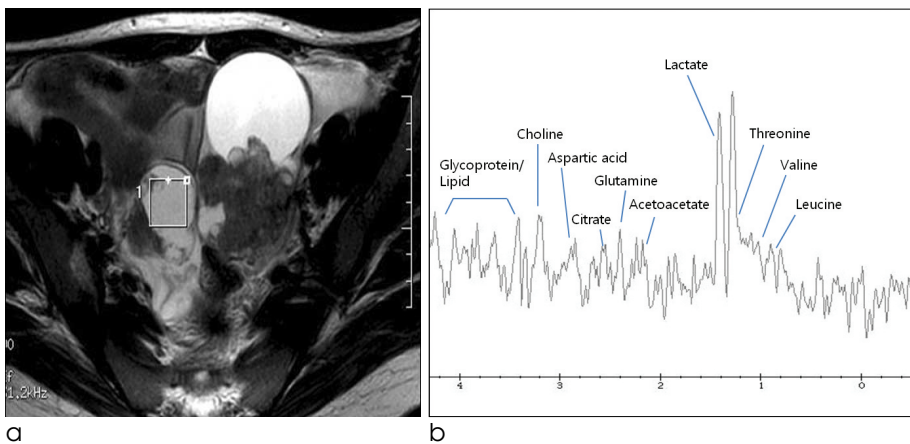


Fig. 5. 44-year-old women with metastatic squamous cell carcinoma (TR=3157 msec, TE=35 msec).

a. Axial T2-weighted MR image shows bilateral ovarian solid and cystic masses.
b. On MRS of cystic portion of right ovarian mass shows double peaks (asterisk) around 1.3ppm.

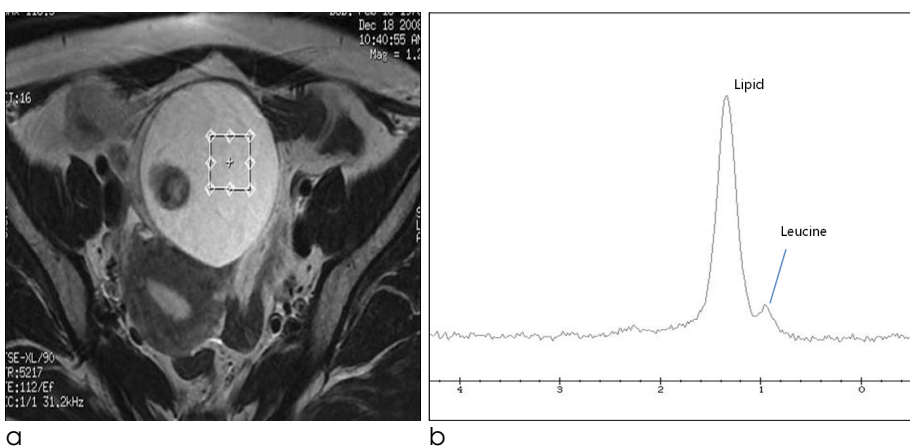


Fig. 6. 31-year-old women with mature cystic teratoma (TR=1500 msec, TE=135 msec).

a. Axial T2-weighted MR image shows a hyperintense cystic lesion containing mural nodule.
b. On MRS, single high peak of lipid (arrow) is detected about 1.3 ppm.

sebaceous component on T2-weighted images is variable, usually approximating that of fat (17, 18). A T1-weighted fat-suppressed sequence distinguished them from hemorrhagic lesion. On MRS, a prominent lipid peak was noted at 1.3 ppm (Fig. 6). A high lipid peak in the mature cystic teratoma was a characteristic finding reflecting a high content of fatty component (10, 19–21). These results may be useful to confirm the histological character of cystic content.

Endometriosis

Endometriosis is classically defined as the presence of functional endometrial glands and stroma outside the uterine cavity. Endometriosis is a common and important clinical problem of women, predominantly those in the reproductive age group. Endometriosis generally occurs within the ovaries and is the result of repeated cyclic hemorrhage. On T1-weighted images, endometriosis has relatively homogenous high signal intensity. Most common and important feature of an

endometrioma is “shading”, which can be seen on T2-weighted images (22, 23). In our four (67%) patients with endometriosis, high lactate double peak was observed in 1.3 ppm, and various lipid and glycoprotein peaks (Fig. 7). Lactate double peak of endometriosis was higher than that of malignant cystic neoplasm (Fig. 1b, c). Massuger et al. (11) detected an unique elevated glycine concentration in endometrial cyst fluid, which corresponds with our finding. Cystic fluid of endometriosis is made in the result of continuous breakdown of components of blood and stromal tissue, and breakdown of cells of stromal part of endometrial tissue may explain the unique elevation of glycine (11). In another two (33%) patients with endometriosis, there were no detectable peaks. This result is comparable to that of Okada et al. (10) and Hascalik et al. (20), which did not find any signal in the spectra of endometrioma, possibly due to the susceptibility of hemosiderin.

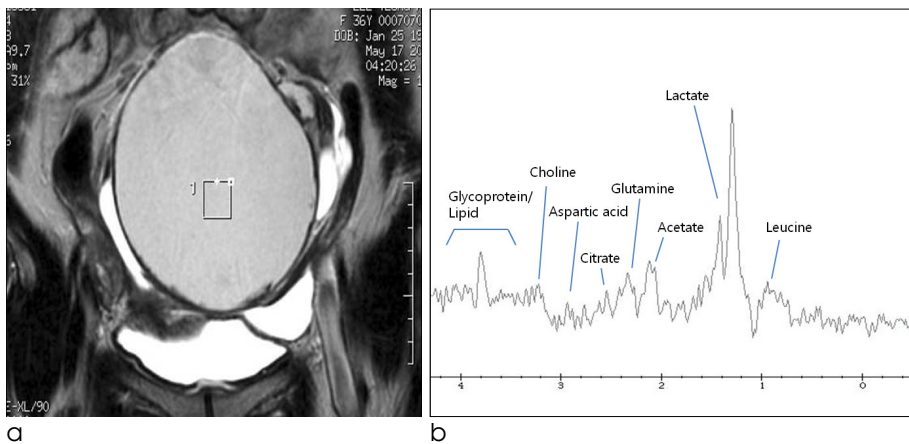


Fig. 7. 38-year-old woman with endometriosis (TR=3157 msec, TE=35 msec).

a. Coronal T2-weighted MR image shows shading in lesions.
b. On MRS, high lipid and lactate peak (asterisk) and glycine peaks (open arrow) are observed.

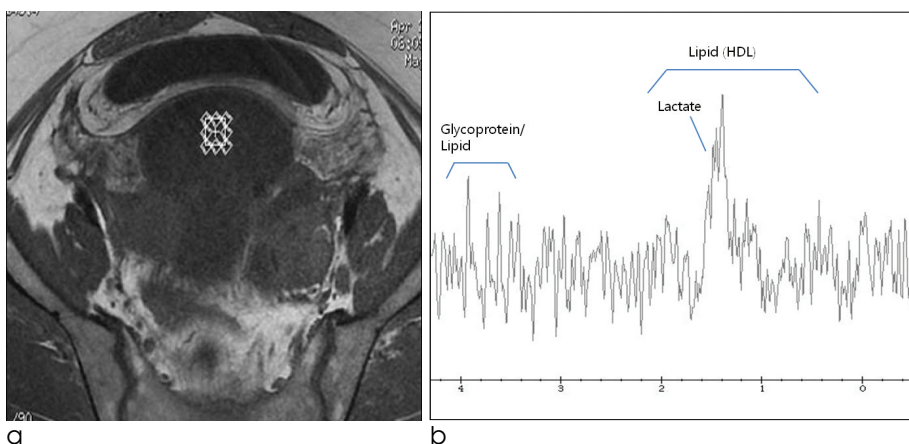


Fig. 8. 48-year-old woman with Tubo-ovarian abscess and pelvic inflammatory disease (TR=1500 msec, TE=30 msec).

a. Axial T1-weighted MR image shows thick-walled cystic lesion in pelvic cavity.
b. On MRS, there is minimal peak (arrow) at 1.3 ppm.

Tubo-ovarian abscess and salpingitis

Tubo-ovarian abscess (TOA) is a late complication of pelvic inflammatory disease. TOA usually occurs in young women but rarely in postmenopausal patients. At MR imaging, TOA usually appears as a pelvic mass with low signal-intensity on T1-weighted images and heterogeneous high signal-intensity on T2-weighted

images. A thin rim of high signal intensity in the inner most portion of the abscess on T1-weighted images is frequently found. Mesh-like strands in the pelvic fat planes due to dense pelvic adhesion or fibrosis are always found (24).

In patient, tubo-ovarian abscess showed lactate, lipid and glycoprotein peaks (Fig. 8) and salpingitis showed

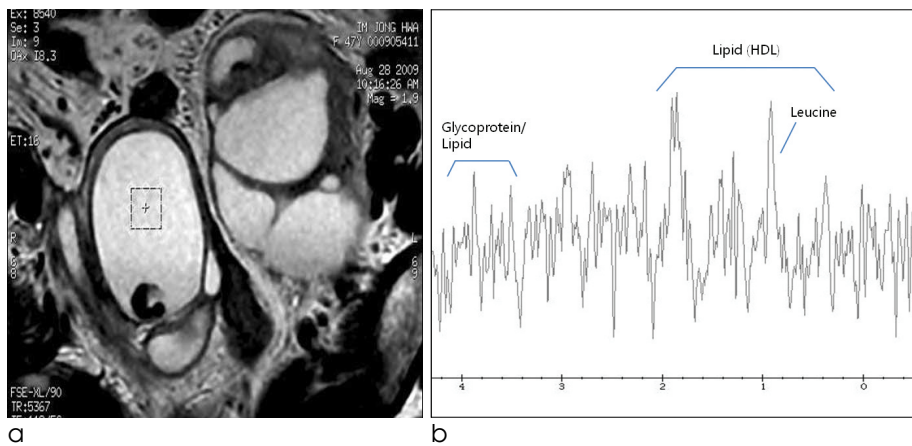


Fig. 9. 47-year-old woman with salpingitis (TR=1500 msec, TE=30 msec).

a. Coronal T2-weighted MR image shows tubular cystic lesions in both adnexa (arrow).

b. On MRS, there is no peak (arrow).

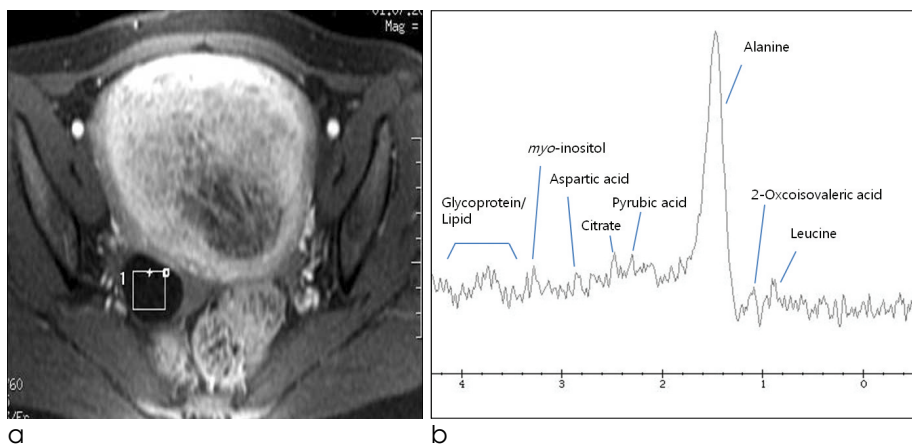


Fig. 10. 37-year-old woman with paratubal cyst (TR=1500 msec, TE=35 msec).

a. Contrast enhanced axial T1-weighted MR image shows thin-walled, unilocular cystic lesion and uterine adenomyosis.

b. On MRS, there is high lipid peak (arrow).

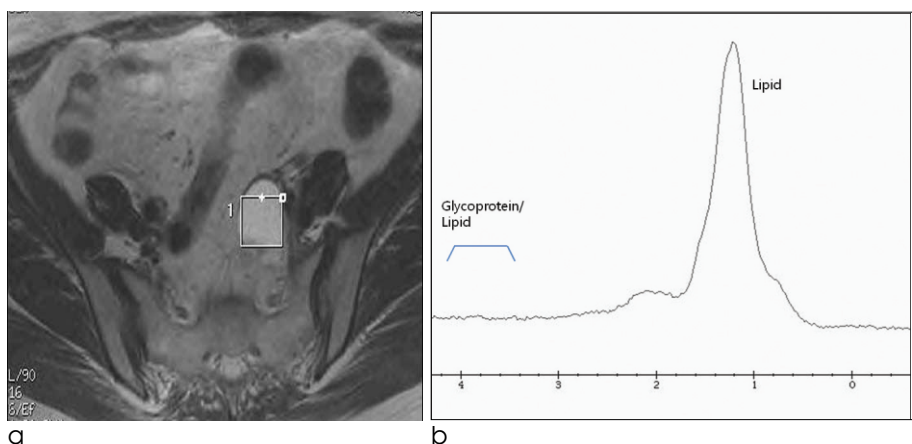


Fig. 11. 48-year-old woman with follicular cyst (TR=3000 msec, TE=35 msec).

a. Axial T2-weighted MR image shows thin-walled, unilocular cystic lesion.

b. On MRS, there is high lipid peak (arrow).

various lipid and glycoprotein peaks (Fig. 9). Lipid and lactate signals were obtained from all patients diagnosed with pelvic abscess in previous study of Hascalik et al.(20). Gotsis et al. reported that MRS demonstrated the presence of lipids in brain abscesses (25). Increased degenerative changes in the pelvic abscesses may lead to considerable cellular deaths, resulting in cellular necrosis, which appears in MRS as a lipid signal. In previous studies, lactate signal was detected in brain abscesses (13, 26). Lactate signal of pelvic abscess represents anaerobic glycolysis as well as hypermetabolic glucose consumption.

Paratubal cyst and follicular cyst

Paratubal cysts of the ovary appear as thin-walled and unilocular adnexal cyst, ranging from 3 to 8 cm in diameter. In our cases, a high single lipid peak was detected in paratubal cyst (Fig. 10) and follicular cysts (Fig. 11). But lipid concentration of follicular cysts was lower than that of dermoid cyst (Fig. 1d, e). Rich lipid content is present in follicular fluid, and our study of this by mass spectrometry is ongoing. The aerobic degradation of the excess of fatty acids is limited by the availability of oxaloacetate, and this will eventually produce a proportional amount of ketone bodies (27). A total of 131 chemical shifts and 42 metabolites were assigned in follicular fluid, including glucose, lactate, acetate, acetoacetate, pyruvate and β -hydroxybutyrate, to be identified (27). High correlations were found between these important intermediaries of the energetic metabolic pathways of the follicle which can indicate the importance of these pathways in oocyte development. Some of these identified metabolites might be useful as biomarkers of the follicular maturation state, allowing oocytes with a higher fertilization potential to be selected, thereby increasing pregnancy rates in women following in vitro fertilization treatments (27). The concentration of lactate is very high in functional follicle and fallopian tube secretions. Thus, lactate could provide an energy supply (perhaps via transformation to pyruvate by the granulosa cells) to the maturing oocyte in the follicle and in the first moments after ovulation (27). More knowledge of the biochemical metabolic composition of ovarian cyst may spur the development of in vivo MRS technique.

CONCLUSION

This article reviews the MRS findings of variable ovarian cystic lesions. MRS may effectively differentiate between benign, malignant tumors and abscess, and additional diagnostic tool for variable ovarian cystic lesions. We conclude that non-invasive proton nuclear magnetic resonance spectroscopy of ovarian cystic lesions can provide valuable information about the presence of low-molecular weight metabolites and evaluate their pathophysiologic mechanisms. Ultimately, MRS may differentiate ovarian tumors, provide useful diagnostic tools and follow-up of patients with ovarian cystic lesions.

Acknowledgment

This work was supported by Inha University research grant.

References

1. Imaoka I, Wada A, Kaji Y, et al. Developing an MR imaging strategy for diagnosis of ovarian masses. *Radiographics* 2006;26:1431-1448
2. Jung SE, Lee JM, Rha SE, et al. CT and MR imaging of ovarian tumors with emphasis on differential diagnosis. *Radiographics* 2002;22:1305-1325
3. Kawamoto S, Urban BA, Fishman EK. CT of epithelial ovarian tumors. *Radiographics* 1999;19 Spec No:S85-102;quiz S263-264
4. Sutton CL, McKinney CD, Jones JE, Gay SB. Ovarian masses revisited: radiologic and pathologic correlation. *Radiographics* 1992;12:853-877
5. Kolwijck E, Engelke UF, van der Graaf M, et al. N-acetyl resonances in in vivo and in vitro NMR spectroscopy of cystic ovarian tumors. *NMR Biomed* 2009;22:1093-1099
6. Mahon MM, Williams AD, Soutter WP, et al. 1H magnetic resonance spectroscopy of invasive cervical cancer: an in vivo study with ex vivo corroboration. *NMR Biomed* 2004;17:1-9
7. Burtscher IM, Holtas S. Proton MR spectroscopy in clinical routine. *J Magn Reson Imaging* 2001;13:560-567
8. Ross B, Michaelis T. Clinical applications of magnetic resonance spectroscopy. *Magn Reson Q* 1994;10:191-247
9. Yoon SH, Park CM, Lee CH, Song IC, Lee HJ, Goo JM. Feasibility of in vivo proton magnetic resonance spectroscopy for lung cancer. *J Korean Soc Magn Reson Med* 2012;16:40-46
10. Okada T, Harada M, Matsuzaki K, Nishitani H, Aono T. Evaluation of female intrapelvic tumors by clinical proton MR spectroscopy. *J Magn Reson Imaging* 2001;13:912-917
11. Massuger LF, van Vierzen PB, Engelke U, Heerschap A, Wevers R. 1H-magnetic resonance spectroscopy: a new technique to discriminate benign from malignant ovarian tumors. *Cancer* 1998;82:1726-1730
12. Park SH, Kim MY, Suh CH, Lee KY, Choi SJ, Cho JY. MR

- Images and ¹H MR spectroscopy of enteric duplication cyst of the pancreas in an adult. *J Korean Soc Magn Reson Med* 2010; 14:139-144
13. Kim SH, Chang KH, Song IC, et al. Brain abscess and brain tumor: discrimination with in vivo H-1 MR spectroscopy. *Radiology* 1997;204:239-245
 14. Mun CW, Cho JY, Shin WJ, et al. Ex vivo proton MR spectroscopy (1H-MRS) for evaluation of human gastric carcinoma. *Magn Reson Imaging* 2004;22:861-70
 15. Hagberg H, Siegbahn A. Prognostic value of serum lactic dehydrogenase in non-Hodgkin's lymphoma. *Scand. J. Haematol* 1983;31:49-59
 16. Boss EA, Moolenaar SH, Massuger LF, et al. High-resolution proton nuclear magnetic resonance spectroscopy of ovarian cyst fluid. *NMR Biomed* 2000;13:297-305
 17. Comerci JT Jr., Licciardi F, Bergh PA, Gregori C, Breen JL. Mature cystic teratoma: a clinicopathologic evaluation of 517 cases and review of the literature. *Obstet Gynecol* 1994;84:22-28
 18. Outwater EK, Siegelman ES, Hunt JL. Ovarian teratomas: tumor types and imaging characteristics. *Radiographics* 2001;21:475-490
 19. Cho SW, Cho SG, Lee JH, et al. In-vivo proton magnetic resonance spectroscopy in adnexal lesions. *Korean J Radiol* 2002;3:105-112
 20. Hascalik S, Celik O, Sarac K, et al. Metabolic changes in pelvic lesions: findings at proton MR spectroscopic imaging. *Gynecol Obstet Invest* 2005;60:121-127
 21. Hascalik S, Celik O, Erdem G. Magnetic resonance spectral analysis of ovarian teratomas. *Int J Gynaecol Obstet* 2005;90:152-154
 22. Woodward PJ, Sohaey R, Mezzetti TP, Jr. Endometriosis: radiologic-pathologic correlation. *Radiographics* 2001;21:193-216;questionnaire 288-294
 23. Bis KG, Vrachliotis TG, Agrawal R, et al. Pelvic endometriosis: MR imaging spectrum with laparoscopic correlation and diagnostic pitfalls. *Radiographics* 1997;17:639-655
 24. Ha HK, Lim GY, Cha ES, et al. MR imaging of tubo-ovarian abscess. *Acta Radiol* 1995;36:510-514
 25. Gotsis ED, Fountas K, Kapsalaki E, et al. In vivo proton MR spectroscopy: the diagnostic possibilities of lipid resonances in brain tumors. *Anticancer Res* 1996;16:1565-1567
 26. Lai PH, Li KT, Hsu SS, et al. Pyogenic brain abscess: findings from in vivo 1.5-T and 11.7-T in vitro proton MR spectroscopy. *AJNR Am J Neuroradiol* 2005;26:279-288
 27. Piñero-Sagredo E, Nunes S, de Los Santos MJ, Celda B, Esteve V. NMR metabolic profile of human follicular fluid. *NMR Biomed* 2010;23:485-495

대한자기공명영상학회지 17:326-333(2013)

남성 난소병변의 자기공명분광술

¹인하대학교 의과대학 인하대병원 영상의학과

²인하대학교 의과대학 인하대병원 병리과학

³인하대학교 의과대학 인하대병원 산부인과학

⁴서울대학교 약학대학

⁵뉴욕대학교 생물학

강영혜¹ · 김미영¹ · 김경태¹ · 김윤정¹ · 서창해¹ · 김준미² · 황성욱³ · 박성혁⁴ · 조재영⁵

¹H 자기공명분광술에서 양성 종양은 양성 병변보다 더 높은 농도의 대사물질들을 보여준다. 락테이트의 이중 첨단 점은 양성 종양과 자궁내막증에서 나타났으며, 자궁내막증에서 더 높은 농도를 보였다. 자궁관난소농양과 난관염은 분명한 첨단점이 보이지 않는다. 유피낭종은 높은 수준의 지질 첨단점이 나타난다. 부난관 낭종 및 난포낭도 지질 첨단점을 보일 수 있지만, 지질의 농도는 유피낭종보다 현저히 낮다. ¹H 자기공명분광술은 남성 난소병변의 대사 물질 성분에 대한 유용한 정보를 제공할 수 있다.

통신저자 : 김미영, (400-711) 인천광역시 중구 인항로 27, 인하대병원 영상의학과
Tel. (032) 890-2769 Fax. (032-890-2743 E-mail: mykim@inha.ac.kr